ATLANTIS PRESS

Advances in Engineering, volume 100

International Conference on Manufacturing Engineering and Intelligent Materials (ICMEIM 2017)

Study on Lubrication Characteristics of Trapezoidal Groove for Planetary Gear Sliding Bearing

Hong-wei Wang *, Kai Huang, and Li-juan Sun

College of Mechanical and Equipment Engineering ,

Hebei University of Engineering, Handan, 056038, China

Keywords: Sliding Bearing, Trapezoidal Groove, Finite Volume Method, Lubrication, Characteristics.

Abstract. It has been proven to be an effective method for reducing the friction and wear of two contact surfaces by introducing a hydrodynamic lubrication mechanism. A linear trapezoidal groove was proposed to accommodate the bidirectional rotation of the planetary gear. Cavitation and fluid rotation centrifugal forces were analyzed by the finite control volume method. The influence of the structural parameters of the groove, such as profile inclination of trapezoidal groove, film thickness ratio, groove number and groove width ratio, on the hydrodynamic lubrication characteristics of the groove were investigated. The results show that an optimal interval value is existent for trapezoidal profile inclination, film thickness ratio and groove number, and simultaneously meeting the maximum bearing capacity and minimum friction coefficient for the fluid lubrication. The cross-sectional area of the groove and rotating centrifugal force have a great influence on the flow rate and cavitation rate of the oil film. When other parameters are unchanged, the trapezoidal profile inclination is better than that of the rectangular groove and the triangle groove in a certain range. The cavitation rate was commonly determined with the oil flow and centrifugal force, but the bearing capacity could be hardly influenced.

Introduction

In the vehicle transmission, the generation of the axial force of the planetary wheel increases the frictional force of the sliding bearing surface of the planetary wheel[1]. When the planetary gears rotate at high speed, the end faces of the sliding bearing would be tilted, which lead to the non-uniform force to it, resulting in that the parts are damaged and become vulnerable components. Radial grooves can generate fluid dynamic pressure between two relatively rotating surfaces, which can offer sufficiently axial load force, according to the theoretical and experimental study of the helical geared thrust bearings in Ref.[2,3]. Yu and Sadeghi[4] analyzed the influence of thrust washer hydrodynamic pressure on lubrication characteristic. The results displayed that groove depth, number of grooves and cavitation has a great influence on the hydrodynamic bearing capacity. The hydrodynamic lubrication characteristics of sliding bearing with radial grooves are studied in detail in literature[5]. The influence of groove edge and groove bottom on the lubrication characteristics of the sliding bearing face is analyzed by Li et al[6]. However, the influence of cavitation on the lubrication characteristics is only focused on the mechanical seal[7-8]. A hybrid genetic algorithm method was applied to optimize the irregular trapezoidal cross-section of the grooved thrust bearing[9]. It is concluded that the bearing capacity of the thrust bearing can be maximized by the specific structural parameters, and when the rectangular section was substituted for the trapezoidal section, the geometric carrying capacity of the groove would be enhanced.

In this study, it was investigated that the influence of the changed structural parameters such as side slope, film thickness ratio, groove number, rotation speed, groove width ratio on the lubrication characteristics including bearing capacity, friction coefficient, cavitation rate and oil flow. The results of the study on the lubricating properties of the trapezoidal groove should provide the theoretical basis for improving the bearing capacity of the oil film on the sliding bearing surface and reducing the wear between the surfaces.

Physical Model

The distributions of linear grooves on the surface of the sliding bearing are periodic. Therefore, when modeling the sliding bearing, a groove area and two adjacent areas should be chosen. The geometry of the groove could be changed by varying the different parameters, and the diagram of the geometric model structure of the sliding bearing groove and the film thickness was shown in Fig. 1.

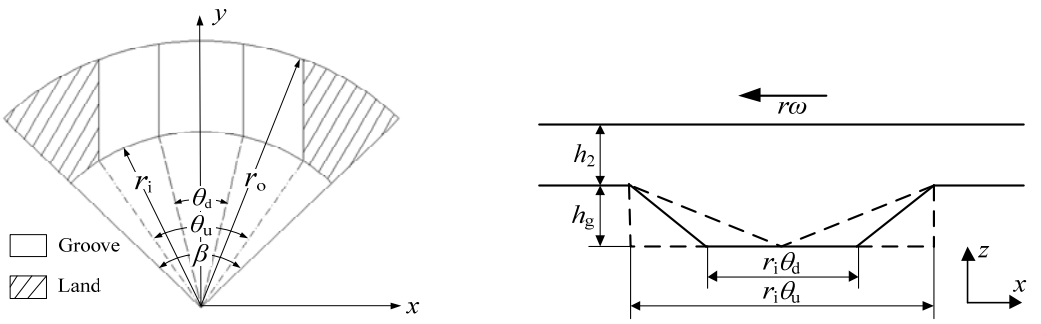

(a)Schematic diagram of sliding bearing groove (b) Film thickness distribution of trapezoidal groove

Figure 1. Physical model of sliding support

Where: ri and ro are the internal and external radius of the sliding bearing, respectively. h2 is the gap of sliding bearing surface and planetary gear working surface. hg is the groove depth. Therefore a groove depth ratio δh=hg/ h2 is defined. □is a central angle occupied by one period. θu and θd are the central angle of the bottom and top edge of the trapezoidal cross-section. δT=θu/θd is defined for the inclination of the trapezoidal cross section, which describe the slope of the side of the trapezoidal groove, and of which the value ranges from 0 to 1. When δT is equal to 0, the groove section is triangular, while δT is equal to 1, the groove section is rectangular.

Mathematical Model

In the numerical analysis of fluid lubrication, the pressure field of the oil film is obtained by the numerical solution of the control equation (Reynolds equation), and the lubricating characteristic parameters such as the bearing capacity and friction coefficient of the oil film are obtained. The derivation of control equations is assumed: (1)Fluid flow is laminar. (2)The fluid viscosity is constant. (3)The sliding bearing surface is parallel with the working surface of the planetary gear, and both of the mare the rigid body. (4)Cavitation occurs only when the liquid film pressure is below the cavitation pressure. (5)The inertial and bulk forces of the fluid are ignored, the effects of centrifugal force is only considered.

Reynolds Equation

Vehicle planetary gear rotation speed is high, with the relative rotational speed, it is assumed that the sliding support is stationary and the rotating disc is rotating at a constant relative speed and fluid inertia term needs to be considered. The control equation with isothermal, laminar flow is given [4]

$$\frac{1}{r}\frac{\partial}{\partial r}\left(\frac{\rho r h^3}{\mu}\frac{\partial p}{\partial r}\right)+\frac{1}{r}\frac{\partial}{\partial \theta}\left(\frac{\rho h^3}{r\mu}\frac{\partial p}{\partial \theta}\right)=6\omega\frac{\partial(\rho h)}{\partial \theta}+\frac{3\omega^2}{10r}\frac{\partial}{\partial r}\left(\frac{\rho^2 r^2 h^3}{\mu}\right) \tag{1}$$

Where: μ is the dynamic viscosity of lubricating oil. ρ is oil density. p is oil film pressure. ω is the rotation angular velocity. h is the oil film thickness.

The boundary conditions for solving the equation are given by the pressure boundary conditions(2) and the periodic boundary conditions(3).

$$p = p_i \text{ at } r = r_i \text{ and } p = p_o \text{ at } r = r_o \tag{2}$$

$$\begin{cases} p(\theta) = p\left(\theta + 2\pi / N_g\right) \\ \left.\dfrac{\partial p}{\partial \theta}\right|_{\theta} = \left.\dfrac{\partial p}{\partial \theta}\right|_{\left(\theta + 2\pi / N_g\right)} \end{cases} \tag{3}$$

In the formula, p_i is input pressure, p_o is output pressure.

Payvar and Salant[10] introduced a modified Reynolds equation developed by Elrod[11] which governs both the full film and cavitation zones. They introduced a function ϕ and a cavitation index F which are defined as

$$F\phi = \frac{p - p_c}{p_a - p_c} \quad \text{in fluid dynamic pressure zone} \tag{4}$$

$$\frac{\rho}{\rho_c} = 1 + (1 - F)\phi \quad \text{in the cavitation zone} \tag{5}$$

Where

$$\begin{cases} F(r,\theta) = 1 & \text{at } \phi \geq 0 \\ F(r,\theta) = 0 & \text{at } \phi < 0 \end{cases} \tag{6}$$

In the formula, pa is oil film reference pressure.

From Eq.(4) to Eq. (6), the universal variable □ and the switching function Fhave its actual physical meaning. In thefull oil film zone F=1,□ is the dimensionless oil film pressure. In the cavitation region F=0, and (1+□) indicates vapor(gas)-liquid mixing ratio.

Dimensionless and substituting Eq.(4) and Eq.(5)in Eq.(1) yields the modified Reynolds equation used in the present work. In order to facilitate the formula is more general, the equation written in vector form

$$\nabla \cdot \left\{ -\bar{h}^3 \nabla(F\phi) + \frac{\mathrm{Re}^* \gamma}{20} \left[1 + (1 - F)\phi\right]^2 \bar{r}\bar{h}^3 \hat{r} + \gamma \bar{r} \left[1 + (1 - F)\phi\right] \bar{h} \hat{\theta} \right\} = 0 \tag{7}$$

Where the dimensionless parameter is defined as

$$\bar{r} = \frac{r}{r_\mathrm{i}} \ , \ \bar{h} = \frac{h}{h_\mathrm{g}} \ , \ \gamma = \frac{6\mu\omega r_\mathrm{i}^2}{(p_\mathrm{a} - p_\mathrm{c}) h_\mathrm{g}^2} \ , \ \mathrm{Re}^* = \frac{\rho_\mathrm{c} \omega h_\mathrm{g}^2}{\mu} \tag{8}$$

The boundary conditions are rewritten as

$$\bar{r} = 1 \text{ at } \phi = \phi_\mathrm{i} \text{ and } \bar{r} = \bar{r}_\mathrm{o} \text{ at } \phi = \phi_\mathrm{o} \tag{9}$$

$$\begin{cases} \phi(\theta) = \phi\left(\theta + 2\pi / N_{\mathrm{g}}\right) \\ \left.\dfrac{\partial \phi}{\partial \theta}\right|_{\theta} = \left.\dfrac{\partial \phi}{\partial \theta}\right|_{\left(\theta + 2\pi / N_{\mathrm{g}}\right)} \end{cases} \tag{10}$$

In Eq.(7), it can be seen that the control equation vector form a passive field with, and the integral in a closed interval (control body) is zero. When the passive field is unrolled, the dimensionless flow through the unit length boundary line can be obtained, which based on the finite control volume method

$$\begin{cases} \overline{q}^{r} = -\overline{h}^{3} \dfrac{\partial (F\phi)}{\partial \overline{r}} + \dfrac{\mathrm{Re}^{*} \gamma}{20} \overline{r} \overline{h}^{3} \left[1 + (1 - F)\phi\right]^{2} \\ \overline{q}^{\theta} = -\overline{h}^{3} \dfrac{\partial (F\phi)}{\overline{r} \partial \theta} + \gamma \overline{r} \overline{h} \left[1 + (1 - F)\phi\right] \end{cases} \tag{11}$$

By integrating the boundary region, the flow through the boundary(r, θ direction) of control body is obtained

$$\begin{cases} \overline{Q}^{r} = \int_{\theta_1}^{\theta_2} \left\{ -\overline{h}^{3} \dfrac{\partial (F\phi)}{\partial \overline{r}} + \dfrac{\mathrm{Re}^{*} \gamma}{20} \overline{r} \overline{h}^{3} \left[1 + (1 - F)\phi\right]^{2} \right\} \overline{r} d\theta \\ \overline{Q}^{\theta} = \int_{\overline{r}_i}^{\overline{r}_o} -\overline{h}^{3} \dfrac{\partial (F\phi)}{\overline{r} \partial \theta} + \gamma \overline{r} \overline{h} \left[1 + (1 - F)\phi\right] d\overline{r} \end{cases} \tag{12}$$

For the vector Eq. (12)the finite volume control method is used in the discretization, and the control volume diagram is shown in Fig. 2. Which contains Ⅰ, Ⅱ, Ⅲ, Ⅳ for the semi-mesh control body region. i, j, respectively, are the number of grid nodes along the directions with r and θ.

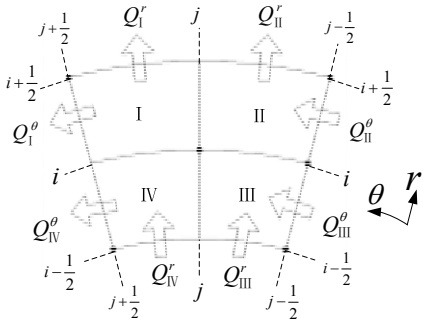

Figure 2. Schematic diagram of control volume

According to the principle of mass conservation, the net flow of fluid flow through the control volume is zero, and the fluid outflow control body boundary is defined as positive.

$$Q_{\mathrm{I}}^{r} + Q_{\mathrm{II}}^{r} + Q_{\mathrm{III}}^{\theta} + Q_{\mathrm{IV}}^{\theta} - Q_{\mathrm{III}}^{r} - Q_{\mathrm{IV}}^{r} - Q_{\mathrm{I}}^{\theta} - Q_{\mathrm{II}}^{\theta} = 0 \tag{13}$$

In order to accurately deal with the abrupt change of the film thickness of the groove area, the value of film thickness at half-step grid is adopted, that is to say, it is necessary to assign accurate values to the left and right hemi-meshes of the abrupt changes in membrane thickness. The integral is calculated of the fluid flow through all boundary of each control body to ensure that the net mass flow rate is zero. It is a foundation that the mass conservation conditions is satisfied to push down the control volume integral discrete format.

Film Thickness Equation

In present study, the bidirectional rotation, rotating sliding supporting with trapezoidal cross section is analyzed. The lower surface of the fluid film is assumed to be perfectly flat and the upper surface is a trapezoidal section groove which can be straight. The geometrical model of the film thickness is first set up in the Cartesian coordinate system, and then converted to the polar coordinate system. Several angles related to the groove boundary are defined.

$$\theta_1=(\pi-\theta_u)/2\ ,\ \ \theta_2=(\pi+\theta_u)/2$$
$$\theta_3=(\pi-\theta_d)/2\ ,\ \ \theta_4=(\pi+\theta_d)/2 \tag{14}$$

The distribution of film thickness in different zones was presented in Fig. 1.

$$\bar{h}=\begin{cases}\bar{h}_2 & r_1\cos(\theta_4)<x<r_1\cos(\theta_3)\\ \dfrac{h_1-h_2}{r_1h_g\left(\cos(\theta_3)-\cos(\theta_1)\right)}|x|+\dfrac{\left(h_2\cos(\theta_3)-h_1\cos(\theta_1)\right)}{h_g\left(\cos(\theta_3)-\cos(\theta_1)\right)} & \text{else}\\ \bar{h}_1 & x>r_1\cos(\theta_1)\ |\ x<r_1\cos(\theta_2)\end{cases} \tag{15}$$

Rectangular coordinate system and polar coordinate system transformation equation

$$\begin{cases}x=r_{i,j}\cos\theta_j\\ y=r_{i,j}\sin\theta_j\end{cases} \tag{16}$$

Numerical Procedure

The first-order upwind scheme is used in the discretization of [1+(1-*F*)] to the diagonally dominant matrix is guaranteed in the computation in reference Ref.[12]. The hysteretic iteration is used for the discretization of the nonlinear terms of $[1+(1-F)]^2$. Therefore, during the iteration, these terms are linearized by lagging the values of ϕ for one iteration step. The discretized dimensionless Eq.(7) with the dimensionless film thickness Eq.(15) form a system of equations that can be solved to using the Gauss-Siedel relaxation scheme.

Firstly, the initial value of F and □ are assigned a value of zero, later, value of Fnew judge by equation (6) after the iterative value of □new obtained by program solution. The values of □ and F are updated by using the relaxed format.

$$\phi_{i,j}^{k+1}=\lambda_\phi\phi_{i,j}^{new}+(1-\lambda_\phi)\phi_{i,j}^{k} \tag{17}$$

$$F_{i,j}^{k+1}=\lambda_F F_{i,j}^{new}+(1-\lambda_F)F_{i,j}^{k} \tag{18}$$

Where

$$\begin{cases}\text{if}\quad \phi_{i,j}^{new}\ge 0\ ,\ \ F_{i,j}^{new}=1\\ \text{if}\quad \phi_{i,j}^{new}<0\ ,\ \ F_{i,j}^{new}=0\end{cases} \tag{19}$$

The present study iteration update factor λ□=0.2~1.2,λF=0.02, meanwhile, the key to the stability of the present method is to use a very small value. In the convergence of the premise of choosing a

larger coefficient can shorten the calculation time. For isothermal solution, the convergence criterion is set at

$$\varepsilon = \sum_{i=1}^{m+1}\sum_{j=1}^{n+1}\left|\frac{\phi_{i,j}^{k+1}-\phi_{i,j}^{k}}{\phi_{i,j}^{k}}\right| \le 10^{-6} \tag{20}$$

When convergence is reached, the cavitation index F is nearly zero in the cavitation region and one in the full film region. After the pressure converges, the fluid lubrication characteristic parameters are calculated.

Hydrodynamic Bearing Capacity

$$W = \left(p_{\mathrm{i}} - p_{\mathrm{c}}\right) r_{\mathrm{i}}^2 \int_0^{2\pi}\int_1^{\bar{r}_{\mathrm{o}}} \left(F\phi - 1\right)\bar{r}\,d\bar{r}\,d\theta \tag{21}$$

Friction Coefficient

$$\mu = \frac{F_f}{W_a} \tag{22}$$

Where, Friction force

$$F_f = h_{\mathrm{g}}(p_{\mathrm{a}} - p_{\mathrm{c}}) r_{\mathrm{i}} \int_0^{2\pi}\int_1^{\bar{r}_{\mathrm{o}}} \left(\frac{\gamma}{6}\frac{\bar{r}}{\bar{h}} + \frac{\bar{h}}{2}\frac{\partial\left(F\phi\right)}{\bar{r}\,\partial\theta}\right)\bar{r}\,d\bar{r}\,d\theta \tag{22}$$

Total bearing capacity

$$W_a = \left(p_{\mathrm{i}} - p_{\mathrm{c}}\right) r_{\mathrm{i}}^2 \int_0^{2\pi}\int_1^{\bar{r}_{\mathrm{o}}} F\phi\bar{r}\,d\bar{r}\,d\theta \tag{23}$$

Volume Flow Rate

$$Q_r = \frac{h_{\mathrm{g}}^3\left(p_{\mathrm{i}} - p_{\mathrm{c}}\right)}{12\mu}\int_0^{2\pi}\left(-\bar{h}^3\frac{\partial\left(F\phi\right)}{\partial\bar{r}} + \frac{\mathrm{Re}^{*}\gamma}{20}\bar{r}\bar{h}^3\left(1+\left(1-F\right)\phi\right)^2\right)\bar{r}\,d\theta \tag{24}$$

Cavitation Ratio

$$\delta_{\mathrm{cav}} = 1 - \frac{\sum_{i=1}^{m+1}\sum_{j=1}^{n+1} F}{\left(m+1\right)\left(n+1\right)} \tag{25}$$

Results and Discussion

The basic parameters in the calculation could be set as follows: r_{i} is equal to16.5 mm, r_{o} is equal to 25 mm, r_{i} is equal to16.5 mm, h_2 is equal to 6μm, h_{g} is equal to 20μm, δ_{T} is equal to 0.5, rotation speed n is equal to 3000r/min, ρ_{c} is equal to 880kg/m^3, p_{i} and p_{o} are equal to 0.1MPa, p_{c} is equal to 0MPa, μ is equal to 0.013Pa·s. For the analysis of lubrication characteristic of oil film, when other parameters are changed, the basic parameters are set and calculated.

Trapezoidal Groove Profile InclinationVariation

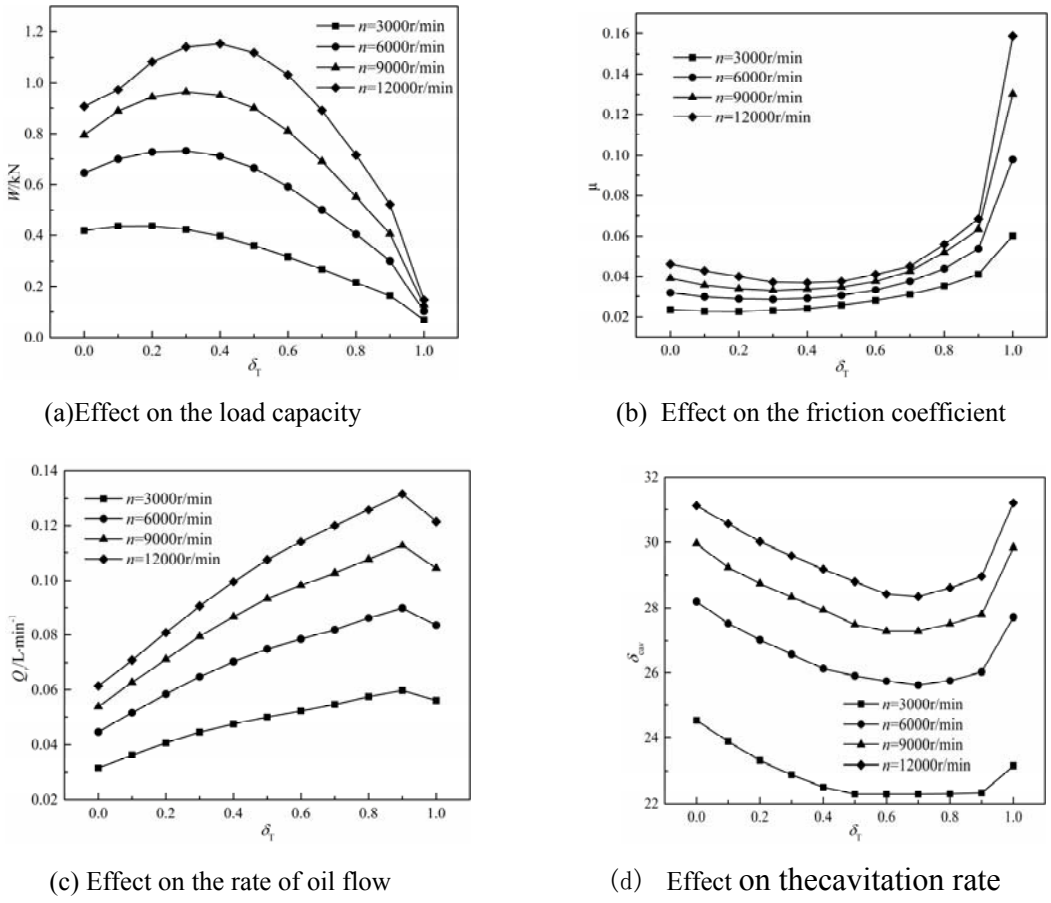

(a)Effect on the load capacity (b) Effect on the friction coefficient

(c) Effect on the rate of oil flow (d) Effect on thecavitation rate

Figure.3 Effect of the groove profile inclination on the lubrication characteristics

Fig. 3 reflects the effect of trapezoidal groove profile inclination on lubrication characteristics of the fluid at different rotational speed. Fig. 3a depicts the effect of the trapezoidal groove profile inclination on the load carrying capacity of the sliding bearing at different rotational speed. The results show that a sliding bearing with a trapezoidal groove on the surface has the stronger ability to support a significant load. At the same rotational speed, δ_T has the most optimal value, which results in the largest bearing capacity of the oil film, and is 0.2 ~ 0.4. The higher the speed of the planet gear is, the stronger the bearing capacity it is, when the other parameters are remained constant. The bearing capacity of the rectangular(δ_T is 1) is less than that ofthe trapezoidal groove. The bearing capacity of the triangular groove(δ_T is 1) is less than the optimal value ofthe bearing capacity of the triangular groove, when the parameters are remained constant. In addition, with the increase of the rotational speed, the bearing capacity of trapezoidal groove is much better. Fig. 3b depicts the effect of the trapezoidal groove profile inclination on the friction coefficient of the sliding bearing surfaces atdifferent rotational speed. Trapezoidal groove profile inclination δ_T has the most optimal value which could results in the smallestsliding bearing surface friction coefficient.The larger the rotational speed, the larger the coefficient of friction. When the other parameters are constant, the friction coefficient of the trapezoidal groove and the triangular groove is smaller than that of the optimal trapezoidal groove. Increased friction coefficient means greater wear and tear consumption, hence friction coefficientof the sliding bearing contact surface should be minimizedin practice. Fig.3c depicts the effect of the trapezoidal groove profile inclination on the rate of oil flow of the sliding bearing at different rotational speed. Larger cross section area and higher speed would lead to larger oil flow rate. Fig. 3d depicts the effect of the trapezoidal groove profile inclination on the cavitation rate of the sliding bearing atdifferent rotational speed. The optimum interval of the groove profile inclination δ_T is 0.5 ~ 0.8, which makesthe smallest cavitation rate of oil film. With the increase of rotational speed, the centrifugal force of the fluid increases, leading to the increase of cavitation rate.

The cavitation rate of both rectangular and triangular grooves are larger than those optimizedvalues ofthe cavitation rate of trapezoidal grooves.

Film Thickness RatioVariation

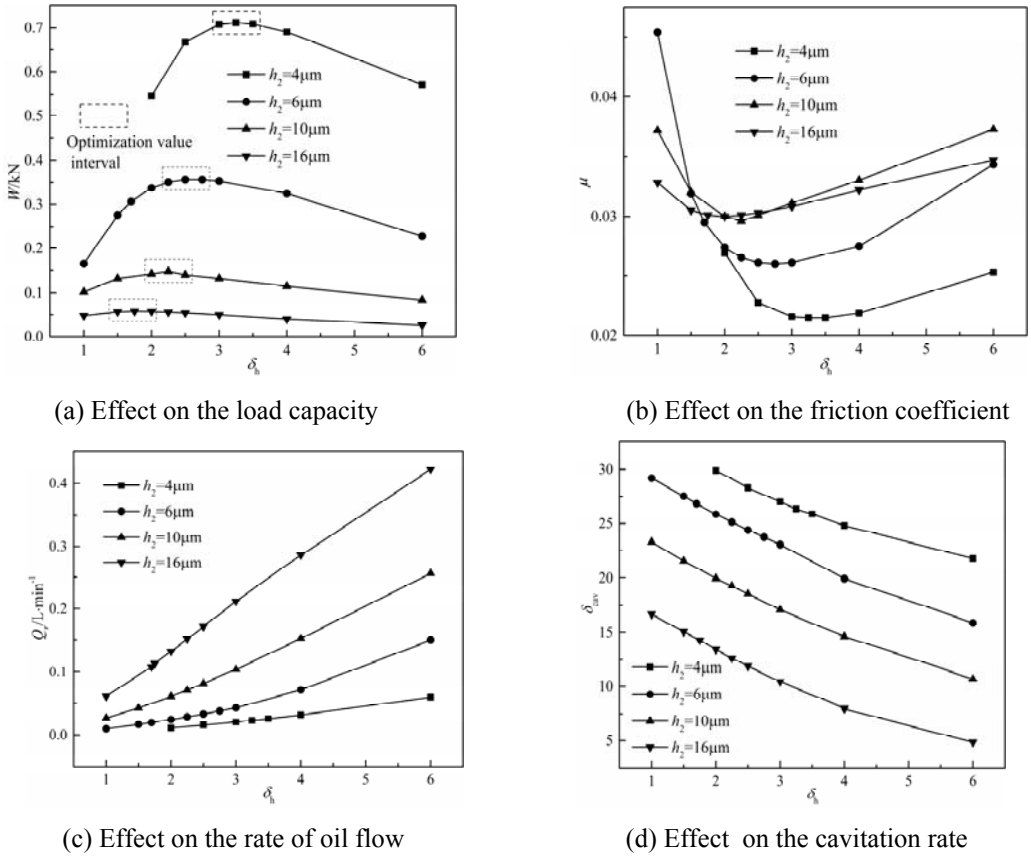

(a) Effect on the load capacity

(b) Effect on the friction coefficient

(c) Effect on the rate of oil flow

(d) Effect on the cavitation rate

Figure.4 Effect of the film thickness ratio on the fluid lubrication characteristics

Fig. 4 reflects the effect of the film thickness ratio δ_h on the fluid lubrication characteristics for different lubrication clearance h_2. Fig. 4a depicts the effect of the film thickness ratio on the load carrying capacity of the sliding bearing for different lubrication clearance. The results show that whenthe end face of planetary gear is different from the surface of the sliding bearing, an optimal value interval is existent, resulting in the largest bearing capacity of the fluid. With the increase of the lubrication clearance, the optimal δ_h would decreases. The smaller the lubrication clearance, the greater the dynamic pressure bearing capacity of the oil film. Fig. 4b depicts the effect of the film thickness ratio on the friction coefficient of the sliding bearing surfaces for different lubrication clearance. The optimum film thickness ratio at different lubrication clearance is existent and would result in the smallestfriction coefficient of the sliding bearing surface. The film thickness ratio have the same optimal interval minimum value in the smallest friction coefficient and largest bearing capacity of the sliding bearing surfaces, when the lubrication clearances are same value. Fig. 4c depicts the effect of the film thickness ratio on oil flow rate for different lubrication clearance. When lubrication clearance value is same, with the increased δ_h, the lubricating oil flow increases linearly. When increasing the lubrication clearance, the increased rate of the lubricating oil flow becomes fast, which is because the cross-sectional area of the groove is proportional to oil flow. Fig. 4d depicts the effect of the film thickness ratio on cavitation rate for different lubrication clearance. As film thickness ratio increase, the cavitation rate of oil film nearly decreased linearly when the lubrication clearance remains unchanged. In addition, the largerlubrication clearance contributes to the smaller cavitation rateof oil film. Therefore, thecavitation rate of oil film can't afford the decisive factor onthe bearing capacity of the factors. The optimal value interval δ_h would lead to the largest fluid

bearing capacity and the smallest friction coefficient. Therefore, when the film thickness ratio is optimized, the cavitation rate of oil film should be minished, if the applied condition has been satisfied.

Groove Number Variation

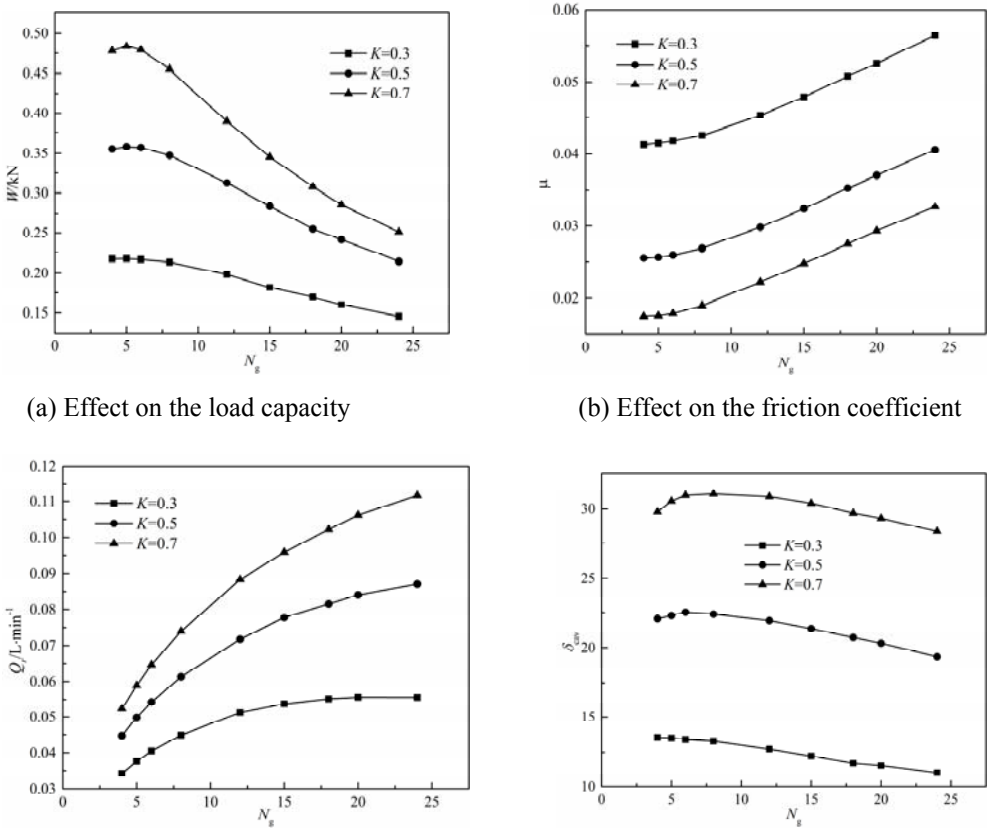

(a) Effect on the load capacity

(b) Effect on the friction coefficient

(c) Effect on the oil flux

(d) Effect on the cavitation rate

Figure.5 Effect of the groove number on the lubrication characteristics

Fig. 5 reflects the effect of the groove number N_g of the lubrication characteristics at different groove width ratio. Fig. 5a depicts the effect of the groove number on the load carrying capacity of the sliding bearing at different groove width ratio. For the number of groove, there is an optimal value, which could maximize the bearing capacity of oil film. When the number of groove is 5, the bearing capacity of the trapezoidal groove is stronger. With the increase of groove width ratio, the bearing capacity of oil film increases gradually. Fig. 5b depicts the effect of the groove number on the friction coefficient of the sliding bearing surfaces atdifferent groove width ratio. When the groove width ratio remains constant, groove number has the best value would result in the smallestfriction coefficient of the sliding bearing surface, and the value of the smallest groove number is the same as the value of the ratio of groove width for obtaining the strongest bearing capacity. When the number of groove is larger than 5, with increase of the groove number, the friction coefficient is increased linearly. In addition, as the ratio of the groove width increases, the coefficient friction would become smaller. Fig. 5c depicts the effect on oil flux at different the ratio of groove width. The flow rate increases with the increase of cross-section area. The groove number increses would lead to, the larger lubricating oil flux, but the increased trend gradually slows down. Fig. 5d depicts the effect of the groove number on cavitation rate at the different ratio of groove width. Cavitation rate increases with the number of groovesincrease at first, then decreases, when the ratio of groove width remains unchanged. Therefore, when the groove number is 6, the cavitation rate reaches the largestvalue. In addition, the greater ratio of groove width would bring larger cavitation rate of the oil film.

Conclusions

In the analysis, δ_T, δ_h and N_g have the same value interval (optimal value), and the strongest bearing capacity and the smallest friction coefficient could be reached in the same condition. When the other parameters are constant, the range of the inclination δ_T of the trapezoidal groove is 0.2 ~ 0.4, the bearing capacity is the largest and the friction coefficient is the smallest. With the increase of the working surface lubrication clearance, the optimal ratio of the film thickness is decreases gradually in the smallest friction coefficient and largest bearing capacity of the sliding bearing surfaces. When the number of grooves is 5, bearing capacity of the sliding bearing surfaces is the largest and the friction coefficient is the smallest. Increasing the rotational speed of the planetary gear, reducing the surface clearance and increasing the ratio of the groove width can increase the bearing capacity of the sliding bearing surface. The flow rate of the lubricating oil is mainly determined by the area of the groove-shaped cross section along the direction of the fluid outlet and the rotational centrifugal force, hence the greater the cross-sectional area and rotation speed, the greater the flow of lubricating oil. The optimum range of inclination of the trapezoidal groove is 0.5 ~ 0.8, in which the cavitation rate of oil film is the smallest. However, the cavitation rate is determined by the flow rate and the centrifugal force of the lubricating oil, and it has no decisive effect on the hydrodynamic bearing capacity. When other parameters remain unchanged, the lubrication characteristics of the triangular and trapezoidal grooves are more superior than that of the rectangular groove. The lubrication characteristics of the trapezoidal groove side in a certain range is better in comparison with that of the triangular groove.

Acknowledgement

This research was financially supported by the National Foundation of Hebei Province, China(E2014402047) .

References

[1] Ju-tao ZHOU, Xiao-jun ZHOU, Fu-chun YANG. Study on Axial Force of Planetary Gear within Compound Planetary Spur Gear Set [J]. Mechanical Engineer, 2010(02):21-24.

[2] Ulezelski J C, Evans D G, Haka R J, et al. NEEDLE BEARING AXIAL THRUST STUDY[J]. Sae Technical Paper, 1983.

[3] Green I. The Behavior of Thrust Washer Bearings Considering Mixed Lubrication and Asperity Contact[J]. Tribology Transactions, 2006,49(2):233-247.

[4] Yu T H, Sadeghi F. Groove Effects on Thrust Washer Lubrication[J]. Journal of Tribology, 2001,123(2):295-304.

[5] Hong-wei WANG, Biao MA, Xi-jing ZHAO, et al. Hydrodynamic lubrication characteristics of planet gear thrust washer used in high- speed planetary transmission [J]. Journal of Drainage and Irrigation Machinery Engineering.2012,30(1):69-74.

[6] Li Yong. Lubrication Characteristics of Planet Gear Axial Sliding Bearings in High—speed Planetary Transmissions of Vehicles [D]. Hebei University of Engineering, 2015.

[7] Ji-bin HU, Ding-hua LIU, Chao WEI. Numerical Simulation for Cavitation of Radial Grooved Face Seals [J].Tribology, 2011,31(6):551-556.

[8] Yi-min ZHAO. Study on Lubricating Condition Prediction and Dynamic Characteristcs of Grooved Rotary Seal ring for Vehicle [D]. Beijing Institute of Technology, 2016.

[9] Papadopoulos C I, Nikolakopoulos P G, Kaiktsis L. Evolutionary Optimization of Micro-Thrust Bearings With Periodic Partial Trapezoidal Surface Texturing[J]. Journal of Engineering for Gas Turbines & Power, 2011,133(1):339-348.

[10] Payvar P, Salant R F. A Computational Method for Cavitation in a Wavy Mechanical Seal[J]. Journal of Tribology, 1992,114(1):199-204.

[11] Elrod H G. A Cavitation Algorithm[J]. Journal of Tribology, 1981,103(3):350-354.

[12] Xiong S, Wang Q J. Steady-State Hydrodynamic Lubrication Modeled With the Payvar-Salant Mass Conservation Model[J]. Journal of Tribology, 2012,134(3):308-314.